TRAMPA HYPERTERMICA DEL RESPLANDOR SOLAR DIRECTO

Piège Hyperthermique du Rayonnement Solaire Direct

(PHRSD)

SYCOMOREEN

SYstems for COnversion of MOtions and REnewable ENergies

systèmes pour la conversion de mouvements et d'énergies renouvelables

NOTA CIENTIFICA

marzo 2008

http://sycomoreen.free.fr

El objetivo de documento actuales lo es to cuantificar las mediciones y las órdenes del tamaño característico de uno PHRSD. El principio de trabajar es explicado abajo :

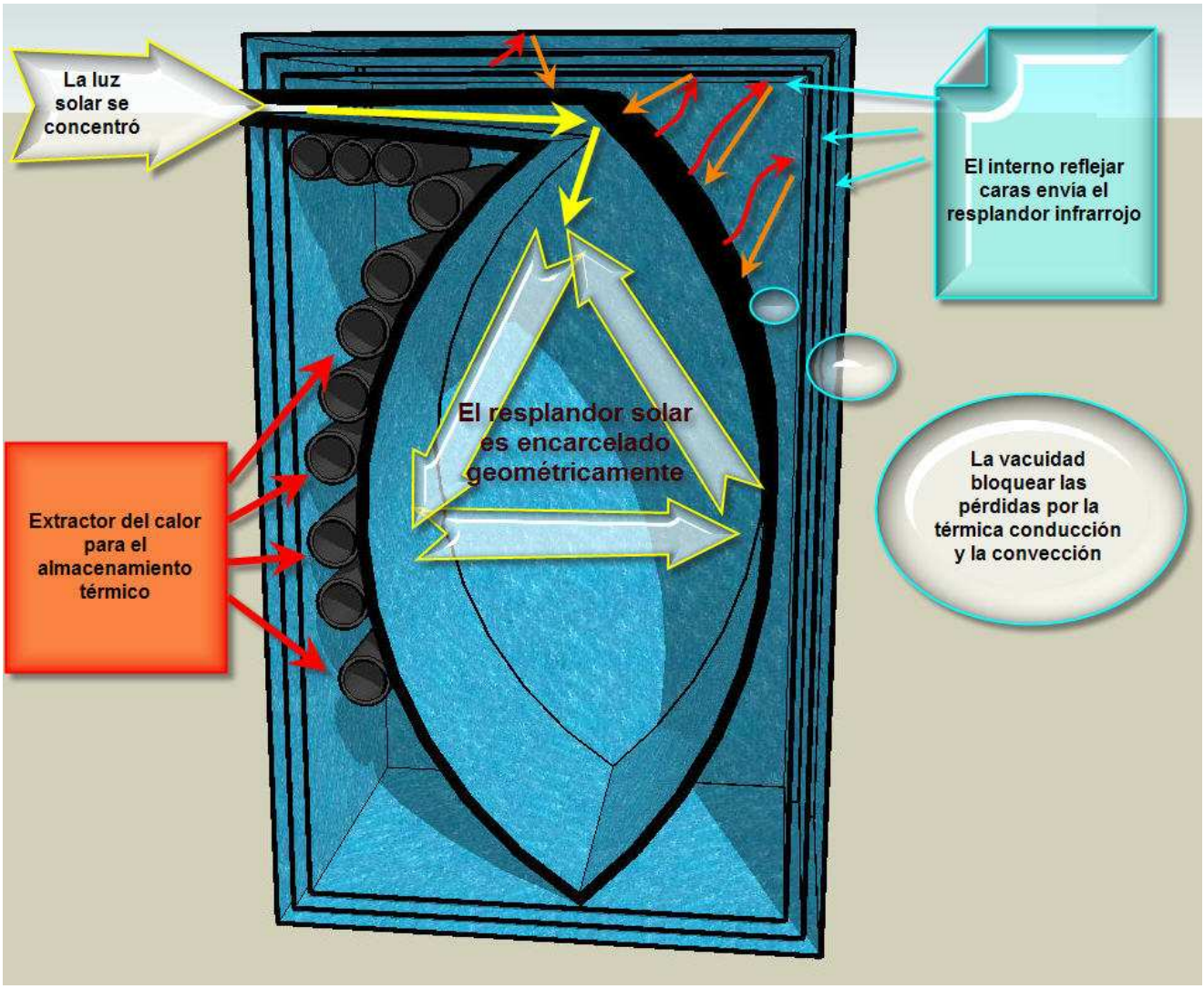

Ilustración amablemente creada por **JMB**, *alias toto65 on www.econologie.com*

Los datos técnicos y las demostraciones son solamente disponible en inglés y en francés, thank you for su conocimiento. Por otro lado, la conclusión de este documento está disponible en español.

Más de los detalles on :

http://sycomoreen.free.fr/syco_espanol/solaire_thermoelec_esp.html

(Traduce en español !)

RESUMEN

1. Measurements

1.1. Measurements of the collecting mirror and outputs

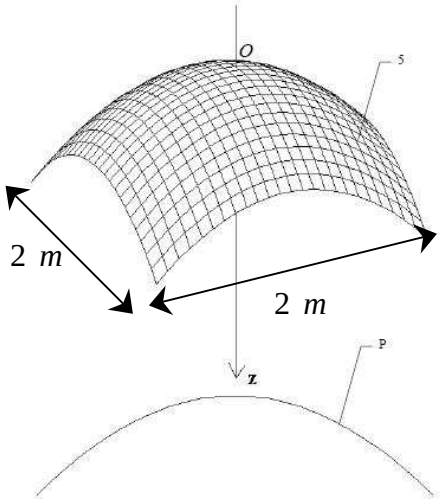

I.1.a) Span and geometrical output

The collecting mirror is a parabolic surface with round or square section of which span is about one meter. We choose here a span $e_{Vg} = 2\ m$ with square section

The collecting surface is thus : $S_C = e_{vg}^2 = 4\ m^2$

However, the energy confining surrounding wall (ECE) and its bearing bars represent a disk of shade of about 30 cm diameter. This diameter brings a shade on the collecting mirror of which the shading radius is $r_m = 0{,}15\ m$. The effective collecting surface is worth therefore : $S_{Ce} = e_{vg}^2 - \pi r_m^2 = 3{,}93\ m^2$

We have here a first geometric output *:* $\eta_{géo} = \frac{S_{Ce}}{S_C} = \frac{e_{vg}^2 - \pi r_m^2}{e_{vg}^2} = 1 - \frac{\pi r_m^2}{e_{vg}^2} = 98{,}23\%$

I.1.b) Focal lentgh and reflexive output

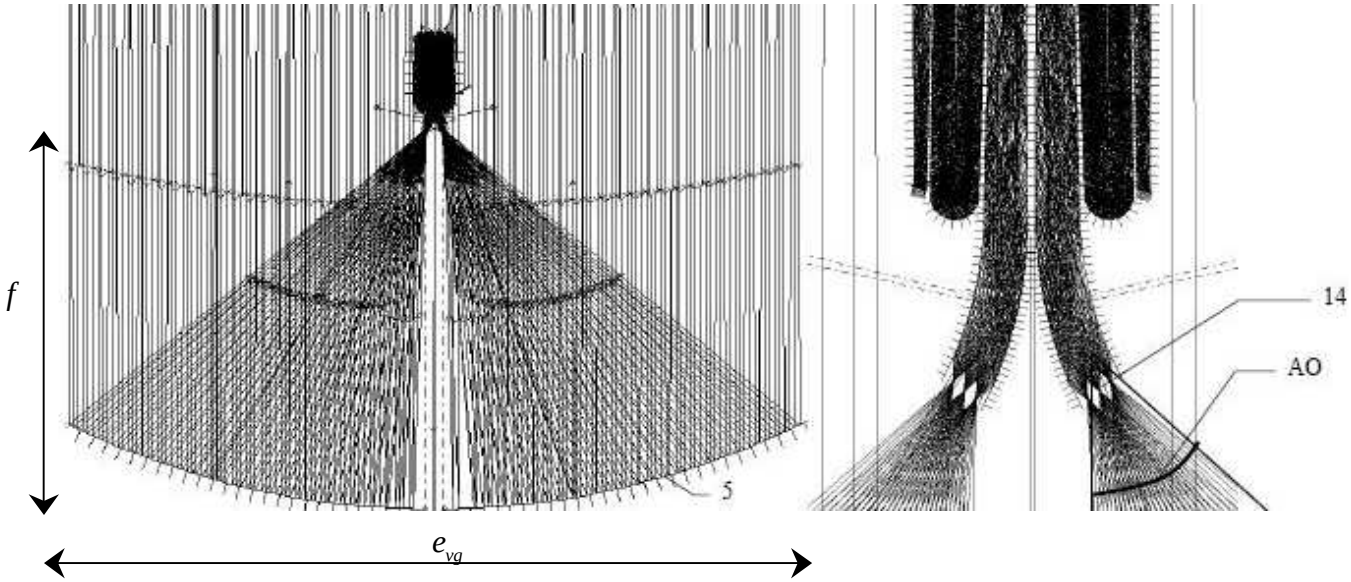

To grant a good penetration in the ECE's opening into the energy confining surrounding wall, the opening angle *AO* of the focused rays must be less or equal to 50°. The equation of a parabola is characterized by a parameter *p* as while calling :

- *z* axial distance relative in the center of mirror
- *r* radial distance relative relative in the center of mirror

the equation writes itself : $z = \frac{r^2}{2p}$

The focal lentgh *f* of the parabola is expressed by $f = \frac{p}{2}$, so that $z = \frac{r^2}{4f}$

Thus, one can express the maximal radius of the mirror corresponding with the distance between its center and one any of its 4 summits : $r_{\max} = \frac{e_{vg}\sqrt{2}}{2}$ Then $\tan AO = \frac{r_{\max}}{f - \frac{r_{\max}^2}{4f}} = \frac{1}{\frac{f}{r_{\max}} - \frac{r_{\max}}{4f}}$

While putting $X = \frac{f}{r_{\max}}$ the ratio characterizing the geometric proportions of the parabola :

$$\tan AO = \frac{1}{X - \frac{1}{4X}}$$

By solving the equation $AO \leq 50°$, one is lead to the condition : $X \geq 1,072$

$$\text{So } f \geq 1.072 \frac{e_{vg}\sqrt{2}}{2} = 0,758\ e_{vg}$$

Thus, we will choose parabolas with f / e_{vg} ratio of about 0,76.

For a 2000 mm span, a focal lentgh ***f = 1600*** **mm** is adequat and gives *AO= 47,68°*.

The reflexive output of the mirror η_{rm} depends on its material and its surface aspect which have to be the smoothest as possible. The silvery mirrors reach 95% of reflexive output, and others made of aluminum 90%. We keep for this study :

$$\eta_{rm} = 90\%$$

I.1.c) Diameter of the sun's image on the focal plan

The theorical diameter D_{Ta} of this image is crucial *because it is the most little opening distance for the entry of the energy confining surrounding wall*. The sun is seen under an angular diameter *DA*=0,52° from the earth so that :

$$D_{Ta}^{théo} = f \tan DA$$

Considering the inhomogeneous light diffusions / refractions in the atmospheric layers, a value *DA = 0,6°* is more applicable, and in this case (*f=1600mm*) :

$$D_{Ta}^{Théo} = 1600 \tan 0.6 = 16,75\ \ mm$$

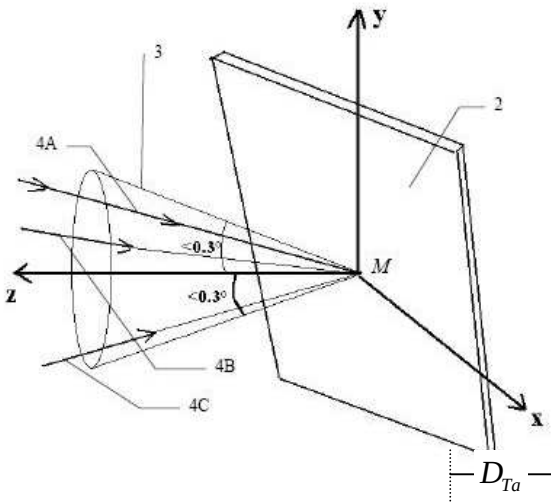

I.2. Measurements of the energy confining surrounding wall (ECE)

I.2.a) Measurements of the entry of ECE

The elaborate current technologies (stars pointing to obtain spectrographic data, or telecommunication satellites) reach angles of pointing imprecision of $\alpha_i \simeq \pm 0,1°$. Some bigger imprecisions (1°) can be corrected by a cone of glass to the entry bringing without losses the rays in the hole by total reflection. On the opposite illustration, the central dark disk represents the site of the solar image in the hypothesis of a perfect sun pointing. The white disks represent the solar image when pointing is imprecise. Δx is the distance corresponding with a pointing imprecision of $|\alpha_i| = 0.1°$. It is thus $\Delta x \simeq f \tan 0,1° = 2,79\ \ mm$

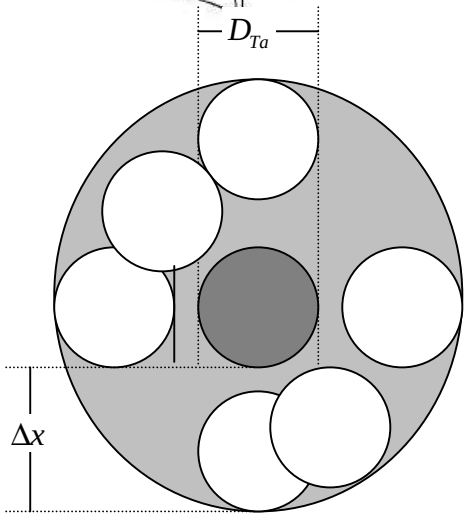

To be sure that all focused rays engulf themselves in the cavity (ECE), its entry diameter *De* must be :

$$D_e = D_{Ta}^{Théo} + 2\Delta x \simeq f\left(\tan DA + 2\tan\alpha_i\right) = 22,34 \ mm$$

The radius of the entry of ECE is worth thus : $r_e = D_e / 2 = 11,17 \ mm$

It means also that the emitive surface offered to the radiance of the cavity is worth :

$$S_e = \pi r_e^2 = 392 \ mm^2 = 3,92 \ cm^2$$

I.2.b) Other measurements

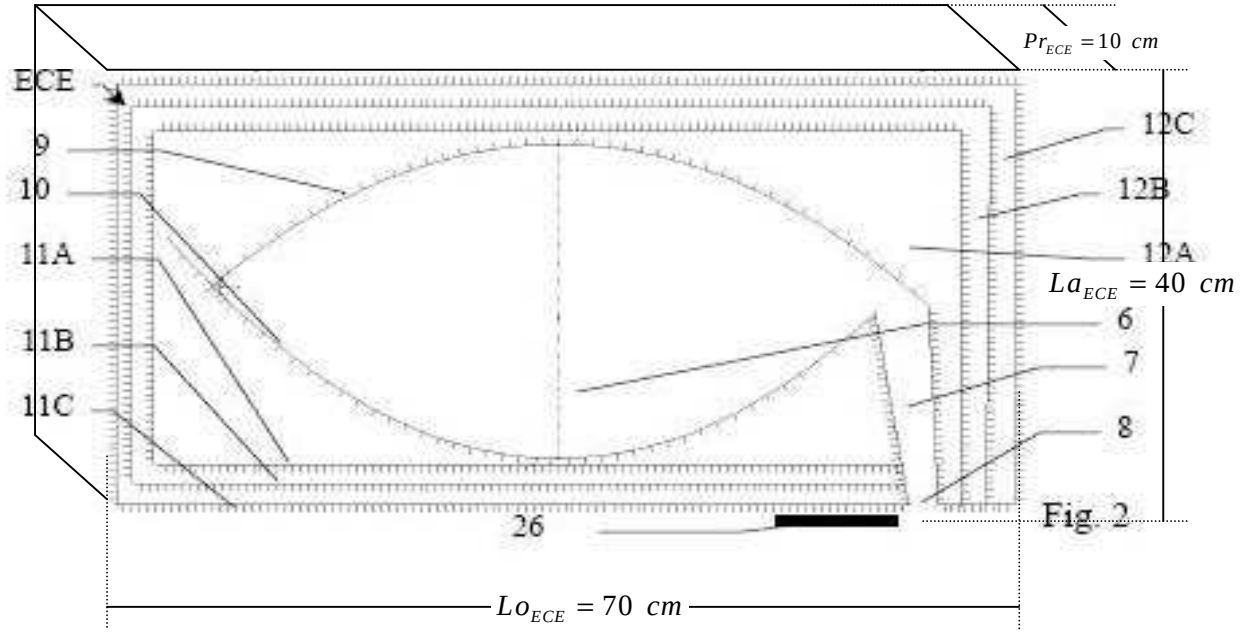

Fig. 2

The face that generates the shade is at the top; its surface is 700 cm² slightly lower than πr_m^2.

Entry diameter is *De*, Small focal lentgh: 125 mm, Long focal lentgh: 150 mm, Distance crossing the cavity: 550 mm.

2. Incoming and retiring powers

2.1. Incoming power

This is the power reflected by the collecting mirror towards the ECE. One call ϕ the incidental solar flux on the mirror (expressed in W/m²). By a very beautiful day without clouds, $\phi \simeq 1200 \ W/m^2$ in France, and much more in meridional zones.

The incidental solar power P_{inc} is given by $\boxed{P_{inc} = \phi S_C}$; in our case, $P_{inc} = 4800 \ W$

The incoming incidental power P_{ie} is obtained by : $\boxed{P_{ie} = \eta_{géo}\eta_{rm}P_{inc}}$ = 4338 W. **It is nearly absorbed completely on the walls of the afocal cavity** because every incoming ray there undergoes average 40 reflections absorbing about 20% of its energy every time : $0,8^{40}$ = 0,013 %, therefore after 40 reflections, only 0,6W not absorbed (very negligible before 4338 W).

2.2. Retiring power

The retiring powers are due to the losses by thermal conduction and radiance (approximately those of a black body). We suppose that the PHRSD is in nominal run, that is to say in *stationary working.*

2.2.a) Retiring thermal conduction powers

The thermal conduction takes place on 2 different areas :

- thermal losses by conduction through the entry of ECE : P_{sce}
- thermal losses by conduction through the sheet metal of insulation separated by vaccuum: P_{sct}

Evaluation of the conduction losses by the entry of ECE

The thermal conductivity of the air λ_{air} at the atmospheric pressure is : $\lambda_{air}^{atm} = 0,0262\ W/m/K$.

One assimilates the entry of ECE to a cylinder of length $L_{ce} \simeq 25\ cm$, of section $S = 1,5S_e = 5,88\ cm^2$. This overcharge by a factor 1,5 simulates the widened character of the anti-return corridor of the bi-concave afocal cavity, of which the temperature T is approximately homogeneous. One put T_{ext} the outside temperature of the atmosphere. Usually $T_{ext} = 20°C = 293\ K$.

One shows in thermal diffusion that the thermal resistance of the entry cylinder is worth : $\boxed{R_{th}^{ce} = \frac{L_{ce}}{\lambda_{air}^{atm} S}}$

And the thermal power lost in stationary working is worth : $\boxed{P_{sce} = \frac{T - T_{ext}}{R_{th}^{ce}}}$

In order of size :

$R_{th}^{ce} \simeq 16228\ K/W$; and if $T - T_{ext} \simeq 1200K$, $P_{sce} = 0,074\ W$

(extremely weak before the incidental 4800 W!)

Evaluation of the conduction losses trough the sheet metal

A low evaluation of the middle thickness of thin air around the bi-concave afocal cavity is :

$$e_{air} \simeq 8\ cm$$

An high evaluation of the interface surface with the atmosphere is :

$$\boxed{S_{atm} = 2\left(Lo_{ECE}La_{ECE} + Lo_{ECE}Pr_{ECE} + La_{ECE}Pr_{ECE}\right)} = 7800\ \text{cm}^2$$

One supposes that the air in ECE has been rarefied sufficiently so that $\lambda_{air}^{iso} = \lambda_{air} / 4$

4 steel surrounding walls come to slow down also this diffusion (but weakly). One puts the thermal conductivity of steel $\lambda_{acier} = 50\ W/m/K$ and the surface of sheet metal $S_{acier} \simeq S_{atm}$, all supposed to be equal (unfavorable hypothesis), and their thickness is $e_{acier} = 5\ mm$.

The thermal resistance of ECE is worth $R_{th}^{ECE} \simeq \frac{e_{air}}{\lambda_{air}^{iso} S_{atm}} + 4\frac{e_{acier}}{\lambda_{air}^{iso} S_{atm}}$

And the thermal power lost in stationary working is worth : $\boxed{P_{sct} = \frac{T - T_{ext}}{R_{th}^{ECE}}}$

By order of size $S_{acier} \simeq S_{atm} = 7800\ cm^2$

$R_{th}^{ECE} \simeq 15.66\ K/W$; et si $T - T_{ext} \simeq 1200K$, $P_{sct} = 76.63\ W$

Also weak power before the incidental power.

2.2.b) Powers of thermal radiance

The thermal radiance takes place on 2 different areas :

- radiance losses through the entry of ECE : P_{sre}
- radiance losses through the insulation sheet metal of ECE : P_{srt}

Preliminary; notion of emitivity

The emitivity ε is a multiplicative factor of the power emitted by a black body : $p_{CN} = \sigma T^4$ W/m²

So that for any body of temperature T of emitivity ε, the radiative real emitted power *p* is

$p = \varepsilon\sigma T^4$ in W/m² with $\sigma = 5,67.10^{-8} W/m^2/K^4$ the Stefan and Boltzmann's constant.

For the polished steel, ε=0,07 to 0,20. We keep $\varepsilon_1 = 0,20$ (the most unfavorable) for the steel undergoing the very high temperature, et $\varepsilon_2 = 0,1$ for the reflective steel of the confining sheet metal.

Evaluation of thermal radiance losses through the entry of ECE

The entry has a surface *Se* which radiates at the temperature *T* : $\boxed{P_{sre} = \varepsilon_1 S_e \sigma T^4}$

Approximate assessment at à 1200 K : 9,21 W (very weak)

Evaluation of thermal radiance losses through the insulating sheet metal

It requires a modelling and enough detailed and complex calculations given in the annex 1. It concludes that : $\boxed{P_{srt} = S_{acier}\sigma\left(F_S T^4 - F_E T_{ext}^4\right)}$ with :

- $F_S = 9.10^{-5}$ the outcoming transmissive factor of radiance (computed for 4 sheet metal)
- $F_E = 0,368$ the incoming transmissive factor of radiance of **diffuse** solar radiance. *The 4 sheet metal* are generating a little greenhouse effect in the ECE due to the absoprtion of the diffuse radiance which makes increase the output of thermal trapping of some % (over of $\eta_{géo}\eta_{rm}$) , especially to the ambient temperature.

3. Outputs of the hyperthermal trap of direct solar radiance (PHRSD)

3.1. Thermal trapping output

This is the ratio η_{th} between the incidental direct radiance power on the collecting mirror and the trapped power inside the energy confining surrounding walls (ECE): $\boxed{\eta_{th} = \dfrac{P_{ie} - P_{sce} - P_{sct} - P_{srt} - P_{sre}}{P_{inc}}}$

3.1.a) Expression

All calculation complete and in relation to the already introduced parameters :

$$\eta_{th} = \eta_{geo}\eta_{rm} - \frac{S_{atm}\sigma\left(F_S T^4 - F_E T_{ext}^4\right) + \varepsilon_1\sigma T^4 S_e + \left(T - T_{ext}\right)\left[\dfrac{S_{atm}}{\dfrac{k_{iso}e_{air}}{\lambda_{air}^{atm}} + 4\dfrac{e_{acier}}{k_r\lambda_{acier}}} + \dfrac{k_S\lambda_{air}^{atm}S_e}{L_{ce}}\right]}{S_C\phi}$$

with in the" median case" (Cf. simulations 3.1.c et 3.3.b):

$S_C = e_{vg}^2$; $\eta_{géo} = 1 - \dfrac{\pi r_m^2}{e_{vg}^2} \simeq 98,23\%$; $S_e = \dfrac{\pi D_e^2}{4}$; $D_e = f\left(\tan DA + 2\tan\alpha_i\right)$

DA=0,6° ; *f=1600 mm* $k_{iso} = 4$; $k_r = 1$; $k_S = 1,5$; $\eta_{rm} \simeq 90\%$

$F_S = T_{4S} = T_{2S}^2 \dfrac{1}{1 - R_{2S}R_{2E}}$ with $R_{2S} = 1 - \dfrac{T_A^2}{4}\dfrac{1}{1 - \left(R_N + \dfrac{T_N}{2}\right)\left(R_A + \dfrac{T_A}{2}\right)}$ et $T_{2S} = \dfrac{T_A^2}{4}\dfrac{1}{1 - \left(R_N + \dfrac{T_N}{2}\right)\left(R_A + \dfrac{T_A}{2}\right)}$

$F_E = T_{4E} = T_{2E}^2 \dfrac{1}{1 - R_{2S}R_{2E}}$ with $R_{2E} = 1 - \dfrac{T_N^2}{4}\dfrac{1}{1 - \left(R_N + \dfrac{T_N}{2}\right)\left(R_A + \dfrac{T_A}{2}\right)}$ et $T_{2E} = \dfrac{T_N^2}{4}\dfrac{1}{1 - \left(R_N + \dfrac{T_N}{2}\right)\left(R_A + \dfrac{T_A}{2}\right)}$

Main piloting parameters of the present modelling :

- e_{vg} : span of the collecting parabolic mirror
- r_m : radius of a disk bringing the same shade as ECE on the collecting mirror
- ϕ : incidental solar flux
- α_i : sun pointing imprecision
- *RA,TA, RN, TN :* reflexion/absorption coefficients of polished steel (A) / brut steel (N)

3.1.b) Optimization of the thermal trapping output

The output is optimized mainly when :

- The collecting surface is big
- The incidental solar flux is big
- The external surface of ECE in contact with the atmosphere is little
- F_E is big, and especially, F_S is little

The global output depends on the temperature and collapse if the temperature T increases too much (influence of T-T_{ext}, **especially** T^4 respectively linked with the conduction/radiance thermal losses).

3.1.c) Simulations

3 cases are going to be presented: unfavorable, median and favorable

1. Unfavorable case

Outside temperature : 20°C
Insulating air **is not** depressurized : k_{iso}=1
The reflecting efficiency on the collecting mirror is 85%
The sun pointing imprecision is 2°
The solar flux **is not** maximal : 900 W/m²

Usual polished and brut steels :
RA=0.9 ; *TA*=0.1 ; *RN*=0.2 ; *TN*=0.8

The results are :
Thermal trapping output :
Rendement de piégeage thermique :

- at 20° : 86,8%
- at 1000°C : 68,8%
- temperature of balance (zero trapping)
    - 2051 K (1778°C)

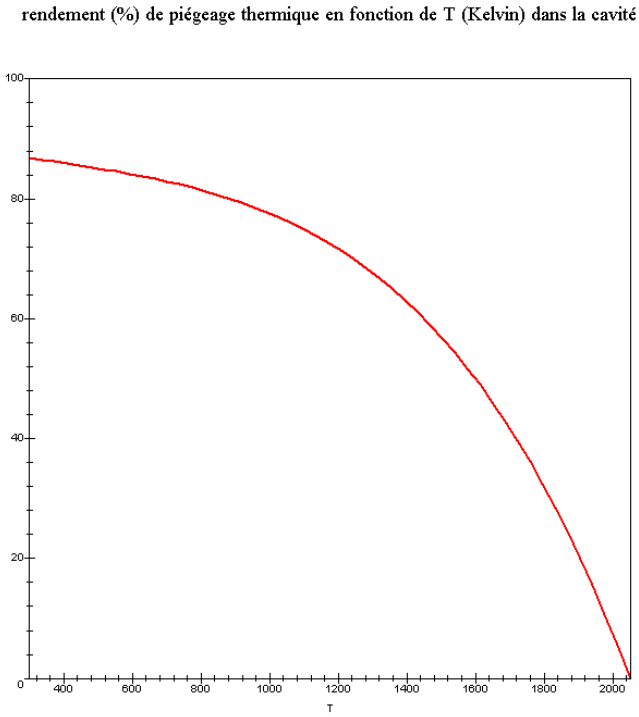

2. Median case

Outside temperature : 20°C
Insulating air **partially** depressurized : k_{iso}=4
The reflecting efficiency on the collecting mirror is 90%.
The sun pointing imprecision is 1°
The solar flux **is good** : 1200 W/m²

Usual polished and brut steels :
RA=0.9 ; *TA*=0.1 ; *RN*=0.2 ; *TN*=0.8

The results are :
Thermal trapping output :
Rendement de piégeage thermique :

- at 20° : 90,9%
- at 1000°C : 86,8%
- temperature of balance (zero trapping)
    - 3011,3 K (2738°C)

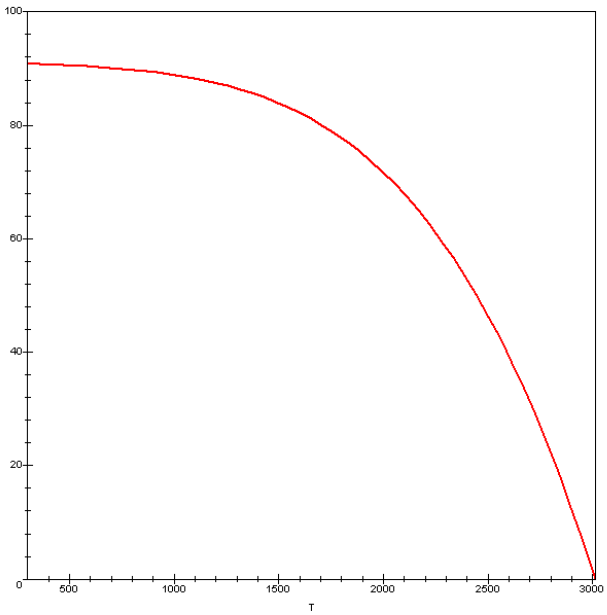

Note : the trap made of steel will support until 1200°C, beyond, it is necessary to use a "high temperature resisting metal or alloy"

3. Favorable case

Outside temperature 20°C
Insulating air **excellently** depressurized
k_{iso}=100
The reflecting efficiency on the collecting mirror is 95%
The sun pointing imprecision is 0.1°
The solar flux **very good** : 1500 W/m²

Very well polished metal, brut and black faces
RA=0.93 ; *TA*=0.07 ; *RN*=0.05 ; *TN*=0.95

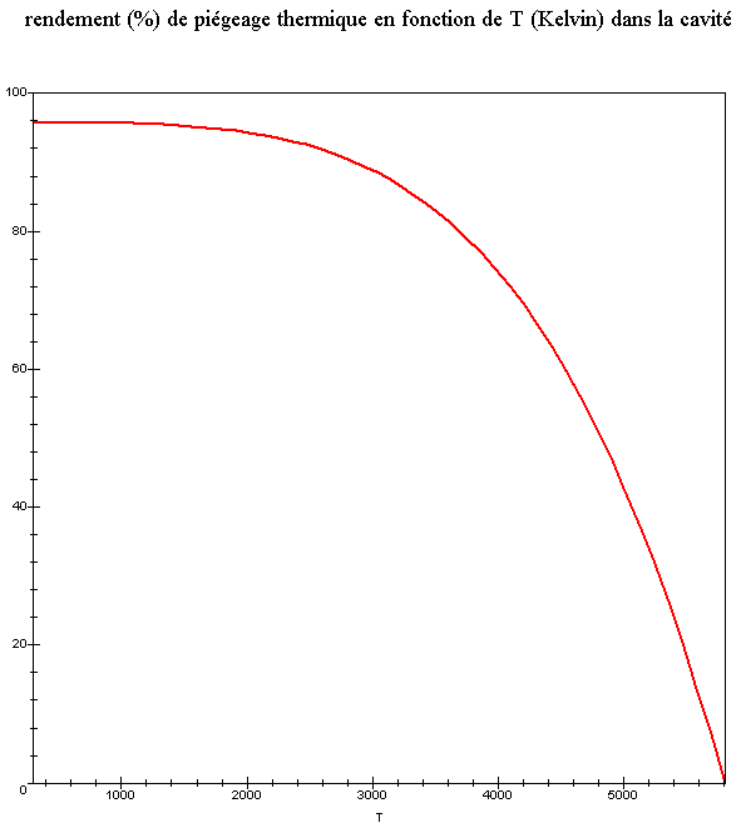

The results are :
Thermal trapping output :
Rendement de piégeage thermique :

- à 20° : 95,8%
- à 1000°C : 95,5%
- temperature of balance (zero trapping)
    - 5807,7 K (5534.7°C)

Note: too elevated temperature. But it is possible to limit themselves to 1000°C or 2000°C and to benefit from the excellent thermal trapping output. **The requisite features are already reachable in the setting of a carelully build realization in desert environment.**

3.2. Output of the thermoelectric machine

The thermoelectric machine consists of a thermodynamic machine, a generator and a converter of injection on the electric network.

3.2.a) Thermodynamic aspect

The considered cycle is a Stirling cycle cooled with the outside and heated temperature by the hyperthermal trap at the temperature *T*. Its theoretical output is the one of Carnot :

$$\eta_C = 1 - \frac{T_{ext}}{T}$$

However, the cycle can make itself with some irreversibilities (mechanical, lamination of fluid.) and thermal flights that we simulate by introducing an irreversible output $\eta_{irrév}$, and finally, the global thermodynamic out put is obtained with :

$$\eta_{thermo} = \eta_{irrév}\eta_C = \eta_{irrév}\left(1 - \frac{T_{ext}}{T}\right)$$

3.2.b Electric output

The electric output $\eta_{élec}$ is the product of the generator's output $\eta_{géné}$ and the injecting on network converter η_{conv}. Finally :

$$\eta_{élec} = \eta_{géné}\eta_{conv}$$

3.3. Global solaroelectric output

3.3.a) Mathematical expression

One put η_{global} the global solaroelectric output. This is the product of the thermoelectric output $\eta_{thermoélec} = \eta_{thermo}\eta_{élec}$ by the thermal trapping output η_{th}. One can have therefore :

$$\boxed{\eta_{global} = \eta_{thermoélec}\eta_{th} = \eta_{thermo}\eta_{élec}\eta_{th}}$$

But more with the 3.1.a) paragraph :

$$\eta_{global} = \left(1 - \frac{T_{ext}}{T}\right)\eta_{irrév}\eta_{géné}\eta_{conv}\left[\eta_{geo}\eta_{rm} - \frac{S_{atm}\sigma\left(F_S T^4 - F_E T_{ext}^4\right) + \varepsilon_1\sigma T^4 S_e + \left(T - T_{ext}\right)\left[\frac{S_{atm}}{\frac{k_{iso}e_{air}}{\lambda_{air}^{atm}} + 4\frac{e_{acier}}{k_r\lambda_{acier}}} + \frac{k_S\lambda_{air}^{atm}S_e}{L_{ce}}\right]}{S_C\phi}\right]$$

3.3.b) Simulations

A very important thing to notice is that the behavior of the thermodynamic η_{thermo} and solar trapping η_{th} *outputs* ***are opposed*** **:**

- at low temperature, η_{thermo} is weak and η_{th} is strong
- at high temperature, η_{th} is weak and η_{thermo} is strong

As the global thermoelectric output is proportional to the product $\eta_{th}\eta_{thermo}$, an optimal temperature T_{opt} is going to clear itself for which the output will reach its maximum. *This temperature is optimal in the sense where it achieves the best compromise of temperature in the objective to produce mechanical work, and therefore possibly electricity.*

We are going to simulate *3 cases*, unfavorable, median and favorable, respectively **according to the 3 cases already presented** on the thermal trapping output. On the following diagrams :

- the green curve represents the thermoelectric output % : $\eta_{thermoélec} = \eta_{thermo}\eta_{élec}$
- the red curve represents the solar trapping output %: η_{th}
- the blue curve represents the global solaroelectric output % : η_{global}

according to the ECE temperature on the horizontal axis.

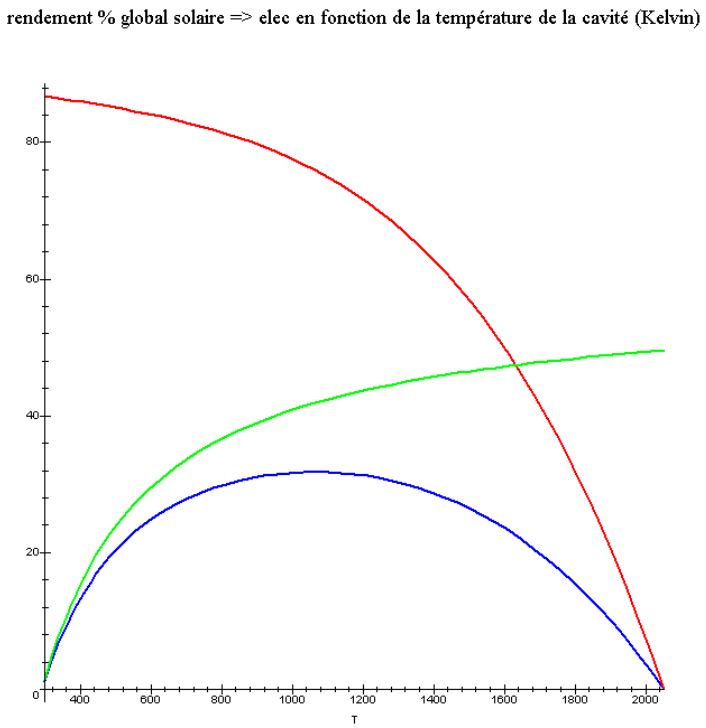

Unfavorable case :

It is represented on the previous curve. The thermodynamic machine presents 20% of irreversibility, either $\eta_{irrév} = 80\%$. The electric generator has an output $\eta_{géné} = 85\%$. The electrical reinjecting converter is quite inefficient: $\eta_{conv} = 85\%$

The calculation shows a maximum output of 30,8% at the temperature of 1062 K, so that T_{opt} =789°C.

Thus, with a material of very middle quality, one reaches the outputs of the best helioelectric present concentrating solar power stations. Let's signal that this performance represents 3 times the one of the photovoltaic with possibility of heat / electricity cogeneration.

Median case :

The material is of appropriate quality: the thermodynamic machine presents 15% of irreversibility, either $\eta_{irrév} = 85\%$. The electric generator has an output $\eta_{géné} = 90\%$. The electric converter is efficient : $\eta_{irrév} = 90\%$

The calculation shows a maximum output of 46,5% with the optimal temperature of 1457 K , so T_{opt} = 1184°.

This performance is perfectly accessible with the material "of the trade" and a trap made of steel. It represents a progression of 50% in relation to the performances of the present power stations.

rendement % global solaire => elec en fonction de la température de la cavité (Kelvin)

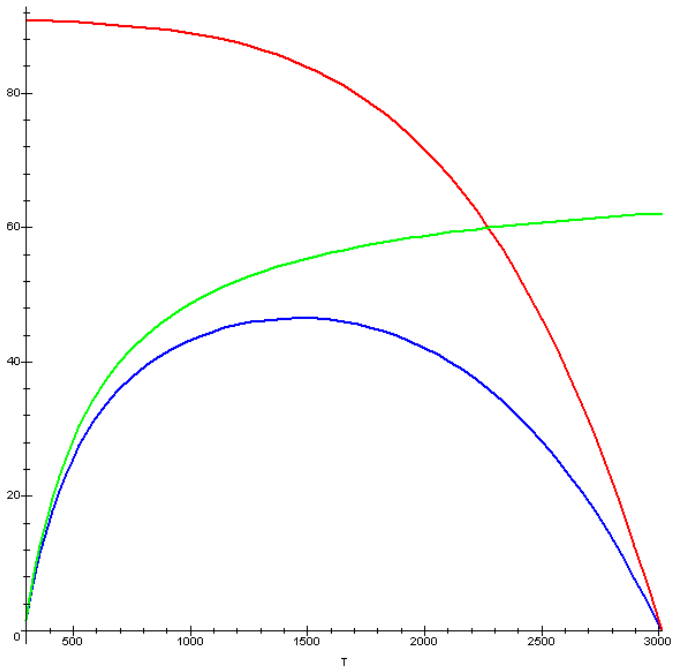

Favorable case :

The material is of superior quality: the thermodynamic machine presents 10% of irreversibility, either $\eta_{irrév} = 90\%$. The electric generator and the converter have excellent behaviours : $\eta_{géné} = 95\%$ and $\eta_{conv} = 95\%$. The trap uses a superheat resistant alloy or metal.

The calculation shows a maximum output of 66,2% at the optimal temperature of 2464K , so that T_{opt} =1991°C. It is the double of the best state of the present art!

This exceptional performance is accessible as using the present best know-how seen in the different domains required by the PHRSD.

rendement % global solaire => elec en fonction de la température de la cavité (Kelvin)

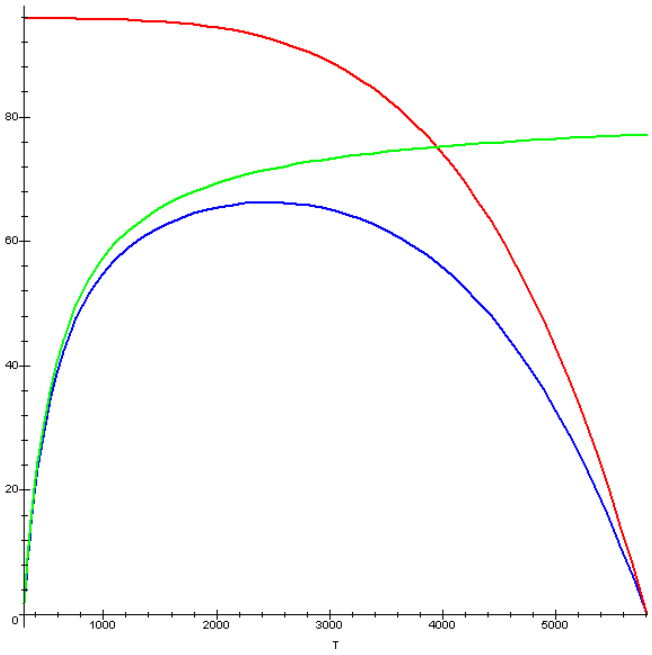

Conclusión

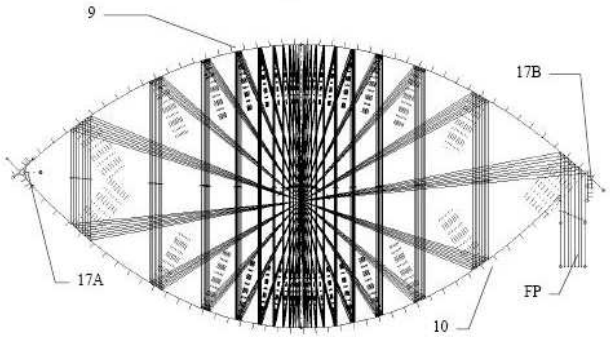

Esta encuesta indicaba *los productos térmicos muy altos y los solaro- eléctrico hecho* posible por **el nuevo concepto de PHRSD :** por un confinamiento geométrico y térmico de la energía solar directa, *el PHRSD es la única máquina capaz llegar a una corriente térmica atrapar el producto de más de 90 % a más de 1000°C*. Permite que él proporcione la energía de la calidad alta a una corriente térmica, se aclarando sobre aplicaciones de *thermolyses*, de *reactor químico ecológico* (para la reacción a lenta cinética de endothermic), y especialmente de la *producción de trabajo mecánica :* en este último caso, el ciclo termodinámico tiene un origen sumamente caluroso y puede llegar a *productos termodinámicos por lo tanto mucho más allá de 50 %*.

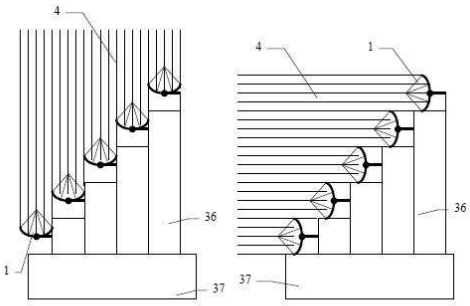

Fig. 15B Fig. 15C

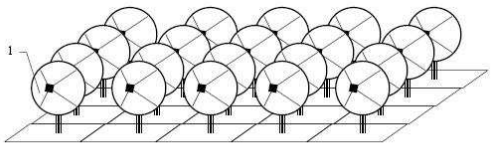

Fig. 15D

Por lo tanto, el PHRSD, sin requerir materiales o saber cómo desconocidos, optimiza todos enlaces de la cadena vigorizante del sol casi hacia la red electrizante : concentración de la luz solar, la confinamiento geométrico, obstrucción de la conducción y la resplandor térmicos, y ciclos definitivamente, termodinámica de la eficiencia alta, notablemente - *de vapor recalentado suministraba energía a los ciclos*, - de Brayton-Joule, pero también y especialmente de *Stirling o Ericsson, cuanto más se adaptar para estirarse hacia el límite de Carnot*.

Él pueden alcanzar solaro eléctrico de los productos hasta aproximadamente 65 % con una comprensión muy ordenada, y 50 % con una construcción de calidad normal, *lo que hace el PHRSD dos veces más fuerte que una central de energía actual* (tecnología de Dish-Stirling o cylindro parabólico espejo) intrínsecamente incompetente hacer el progreso sus eficiencia en tales proporciones sin ser optimizados por el PHRSD.

Indudablemente, ***el PHRSD puede causar una contribución enorme e inagotable de la energía renovable***, *centralizado también que se descentralizó* ***en las mezclas vigorizantes***. Solamente más otra vez, *el PHRSD podía hacerse tal vez la tecnología que permite la difusión enorme de los nuevos vectores vigorizantes* quien es solamente limpio a la condición de proveer una corriente térmica muy importante y renovable y/o la energía eléctrica: así que hidrógeno, los combustibles descendidos de los biomass (por la pausa térmica, licuefacción (CTL, BTL.) o thermolyses), productores de électro positivos de metales de hidrógeno by el contacto con agua (sodio, aluminio) encontró a una fuente vigorizante capaz tal vez allí para empezar su desarrollo intencionadamente.

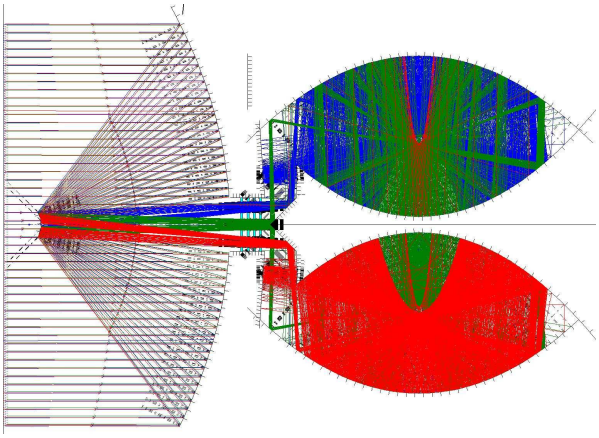

En conclusión, *mientras se apoyar sobre el poder y la abundancia de la energía solar, y mientras explotar elementos perfectamente conocidos en los dominios de la física y la tecnología, el PHRSD es una avant gardist de solución y viable al cortocircuito el término. Solamente algunas sociedades colectivas industriales revelarán su potencialidades numerosas y estratégicas sus ya bien completamente* a la hora de entrar en climático calor y los dependences vigorizantes demasiado poderoso (el gas, el aceite) que van a intensificarse peligrosamente en un futuro cercano (el « Peak-Oil »).

Precisions y contact on http://sycomoreen.free.fr

ANNEX 1 : **Transmissive factors of the thermal radiance for the 4 sheet metal**

Modelling

The ECE has an outside surface S_{acier} and its losses will be considered as those of 4 sheet metal with a surface equal to S_{acier}. The stake of this calculation is to value for 4 sheet metal:

- F_S the *outcoming transmissive factor of the radiance of the trap,*
- F_E the *incoming transmissive factor of the outside diffuse solar radiance* (warning : no link with the collected radiance by the concentrating mirror).

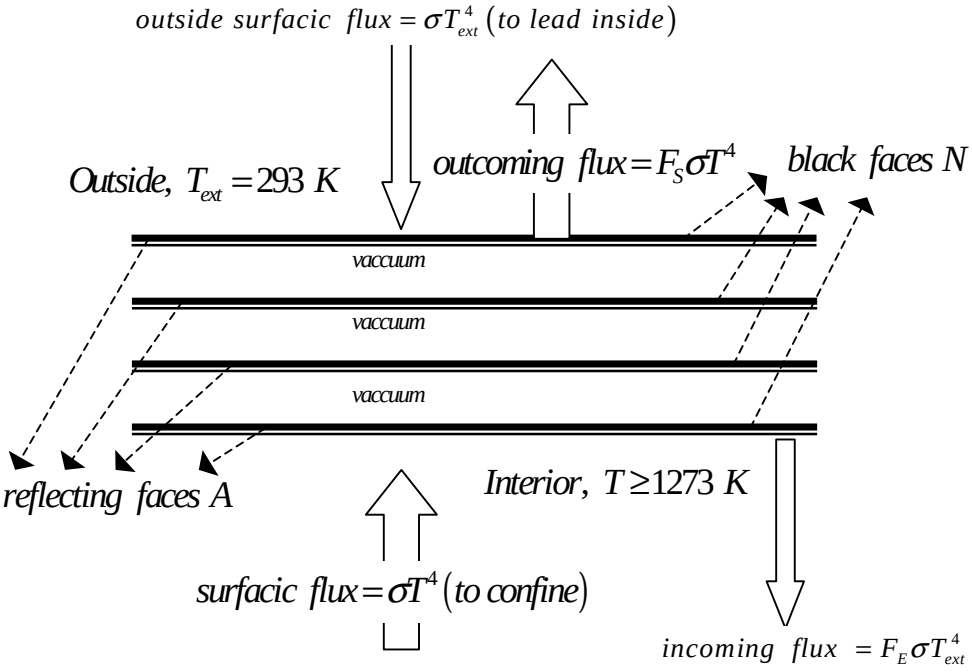

The fluxes to confine and to make go back are roughly radiances of black body. At 1000°C, either 1273 K, the law of the displacement of Wien indicates us the major lengths of wave $\lambda_{pS}, \lambda_{pE}$ of these radiances ;

$$\lambda T = 2898 \mu m.K \Rightarrow \quad \boxed{\lambda_{pE} \simeq \frac{2898}{1273} = 2,27 \mu m} \text{ et } \boxed{\lambda_{pE} \simeq \frac{2898}{293} = 9,89 \mu m}$$

In these domains linked with *the near and far infrared radiances :*

- The reflecting/transmitting factors for energy of any brut steel face are :

$$R_N = 0,2 \; ; T_N = 0,8$$

- The reflecting/transmitting factors for energy of any polished steel (or silvered) face are :

$$R_A = 0,9 \; ; T_A = 0,1$$

One supposes a stationnary working : thus the sheet metal have constant temperatures and don't store the absorbed radiance. They are also supposed to reemit equally the radiance on their 2 faces. The elementary energizing balance of an impact on a sheet metal is therefore the next one for a "unit energy" of impact :

Outcoming impact

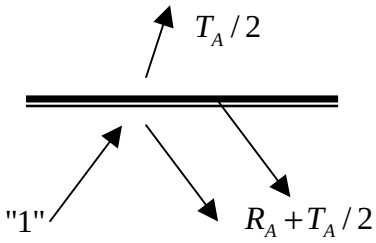

Incoming impact

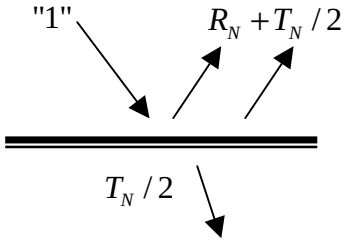

The successive reflections/absorptions/re-emissions are leading to the folowing schematic representation :

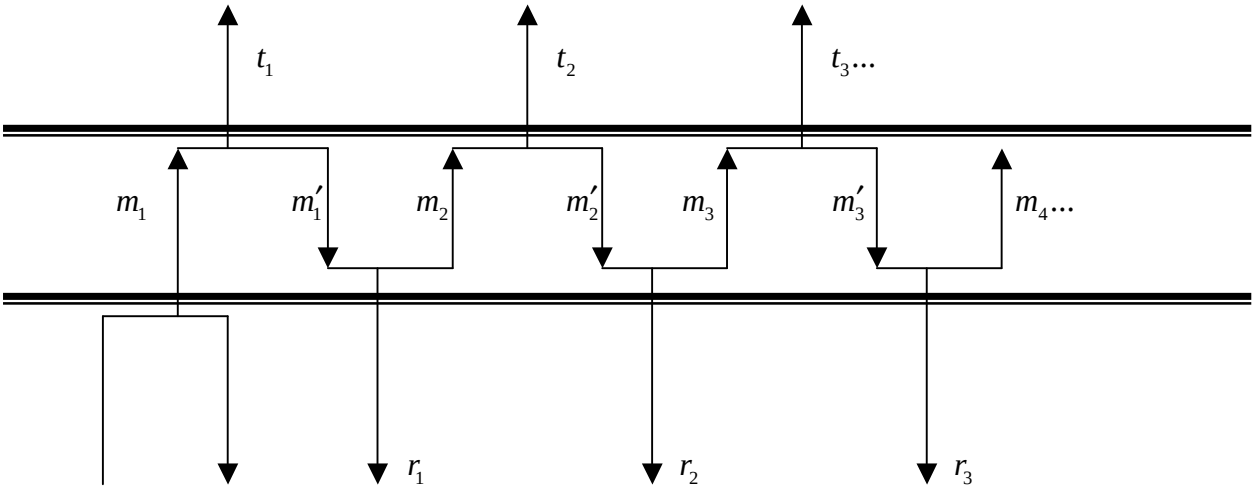

With the recursive continuations, from the unit energy "1" :

- m_n representing the fraction of energy in the outcoming sense at the end of the n-th cycle
- m'_n representing the fraction of energy in the incoming sense at the end of the n-th cycle
- r_n representing the fraction of energy confined after the n-th cycle
- t_n representing the fraction of energy transmitted after the n-th cycle

In relation to the previously exposed energizing balances, it gives the following relations $\forall n > 1$*:*

$$t_n = \frac{T_A}{2} m_n \qquad m'_n = \left(R_A + \frac{T_A}{2} \right) m_n \qquad r_n = \frac{T_N}{2} m'_n \qquad m_{n+1} = \left(R_N + \frac{T_N}{2} \right) m'_n$$

These four relations give the recursive definition :

$$\boxed{m_{n+1} = \left(R_N + \frac{T_N}{2} \right)\left(R_A + \frac{T_A}{2} \right) m_n}$$

One puts $q = \left(R_N + \frac{T_N}{2} \right)\left(R_A + \frac{T_A}{2} \right)$ the geometric factor of this recursive continuation :

It leads immediately to $\boxed{m_n = q^{n-1} m_1}$ with $m_1 = \frac{T_A}{2}$

Therefore, one can put and deduct T_{2S} the *outcoming transmissive factor* of 2 sheet metal :

$$T_{2S} = \sum_{k=1}^{\infty} t_k = \frac{T_A}{2} \sum_{k=1}^{\infty} m_k = \frac{T_A}{2} \sum_{k=1}^{\infty} q^{k-1} m_1 = \frac{T_A^2}{4} \sum_{j=0}^{\infty} q^j = \frac{T_A^2}{4} \frac{1}{1-q}$$

And finally, $\boxed{T_{2S} = \frac{T_A^2}{4} \frac{1}{1 - \left(R_N + \frac{T_N}{2} \right)\left(R_A + \frac{T_A}{2} \right)}}$ *typical value : 5,814.10^{-3}*

One deducts from it, by applying the princip of the energy's conservation, *the outcoming confining factor* R_{2S} for 2 sheet metal :

$$\boxed{R_{2S} = 1 - T_{2S} = 1 - \frac{T_A^2}{4} \frac{1}{1 - \left(R_N + \frac{T_N}{2} \right)\left(R_A + \frac{T_A}{2} \right)}}$$ typical value : 0,9942

Let put now : *(annexe 1 continuation)*

- T_{2E} the incoming transmissive factor for 2 sheet metal :
- R_{2E} the incoming confining factor for 2 sheet metal :

They deduct themselves without supplementary calculation by the permutation of the indices N et A, so that :

$$T_{2E} = \frac{T_N^2}{4} \frac{1}{1-\left(R_A + \frac{T_A}{2}\right)\left(R_N + \frac{T_N}{2}\right)}$$

nearly 0,372

$$R_{2E} = 1 - T_{2E} = 1 - \frac{T_N^2}{4} \frac{1}{1-\left(R_A + \frac{T_A}{2}\right)\left(R_N + \frac{T_N}{2}\right)}$$

nearly 0,628

4 sheet metal case calculations

The four sheet metal react as if it were a superposition of 2 systems based on 2 sheet metal. Each system of 2 sheet metal is working for an elementary impact as described below :

Outcoming impact,

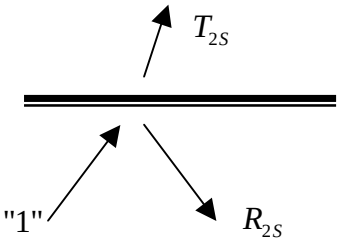

Incoming impact

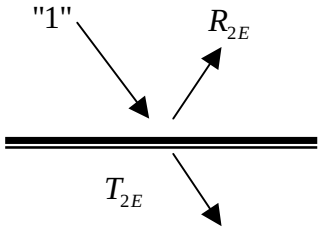

The successive reflexions/transmissions lead to the following schematic representation :

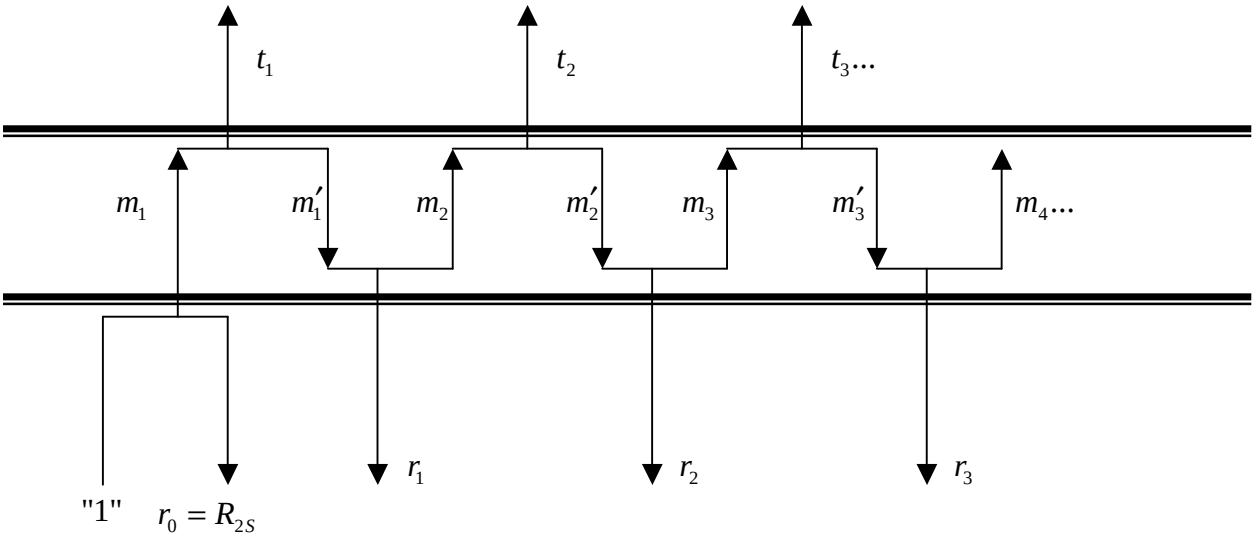

With the recursive continuations, from the “unit energy” :

- m_n representing the fraction of energy in the outcoming sense at the end of the n-th cycle
- m'_n representing the fraction of energy in the incoming sense at the end of the n-th cycle
- r_n representing the fraction of energy confined after the n-th cycle
- t_n representing the fraction of energy transmitted after the n-th cycle

In relation to the previously exposed energizing balances, it gives the following relations $\forall n > 1$*:*

$t_n = T_{2S} m_n$ $\quad$ $m'_n = R_{2S} m_n$ $\quad$ $r_n = T_{2E} m'_n$ $\quad$ $m_{n+1} = R_{2E} m'_n$

These 4 relations bring the recursive continuation :

$$\boxed{m_{n+1} = R_{2E} m'_n = R_{2E} R_{2S} m_n}$$

One puts $Q = R_{2E} R_{2S}$ the geometric factor of this recursive relation :

It comes immediately $\boxed{m_n = Q^{n-1} m_1}$ with $m_1 = T_{2S}$

Therefore, one can put and deduct T_{4S} *the outcoming transmissive factor* of 4 sheet metal :

$$T_{4S} = \sum_{k=1}^{\infty} t_k = T_{2S} \sum_{k=1}^{\infty} m_k = T_{2S} \sum_{k=1}^{\infty} Q^{k-1} m_1 = T_{2S}^2 \sum_{j=0}^{\infty} Q^j = T_{2S}^2 \frac{1}{1-Q}$$

And finally, $\boxed{T_{4S} = T_{2S}^2 \frac{1}{1 - R_{2S} R_{2E}}}$ $\quad$ *typical value : 9.10*$^{-5}$

By applying the energy's conservation princip, it leads to R_{2S} *the outcoming confining factor* for 4 sheet metal :

$$\boxed{R_{4S} = 1 - T_{4S} = 1 - T_{2S}^2 \frac{1}{1 - R_{2S} R_{2E}}}$$ typical value : 0,99991

Let put now :

- T_{4E} the incoming transmissive factor for 2 sheet metal,
- R_{4E} the incoming confining factor for 2 sheet metal :

Without additional calculation, they come from the permutation of the indices S and E, so that :

$$\boxed{T_{4E} = T_{2E}^2 \frac{1}{1 - R_{2E} R_{2S}}}$$ nearly 0,368

$$\boxed{R_{4E} = 1 - T_{4E} = 1 - T_{2E}^2 \frac{1}{1 - R_{2E} R_{2S}}}$$ nearly 0,631

<u>Overview of the 4 sheet metal insulation relative to radiance</u>

Permanently, the 4 insulating sheet metal, from the afocal biconcave cavity's point of view :

- make the cavity lose the radiance : $T_{4S} \sigma T^4 S_{acier}$
- make the cavity gain the radiance : $T_{4E} \sigma T_{ext}{}^4 S_{acier}$

Finally, one can easily identify the searched factors :

$$\boxed{F_{4S} = T_{4S} = 0,00009}$$ et $$\boxed{F_E = T_{4E} = 0,368}$$

ANNEX 2 : some emitivities relative to materials and their surface aspect

Source : Raytek Corporation 1999 – 2008, http://www.raytek.fr/ infrared temperatures measurement without contact

En tout rigueur, les émissivités dépendent de la longueur d'onde à laquelle on effectue la mesure.

Matériel	**Emitivity** ε with $\phi_{emitted} = \varepsilon_\lambda \sigma T^4$		
	$\lambda =$ **1,0 µm**	$\lambda =$ **1,6 µm**	$\lambda =$ **8-14 µm**
Aluminum			
non oxydé (non oxidized)	0,1-0,2	0,02-0,2	n. d.
Oxydé (oxidized)	0,4	0,4	0,2-0,4
Alliage A3003 (alloy)			
Oxydé	n. d.	0,4	0,3
Rugueux (rough)	0,2-0,8	0,2-0,6	0,1-0,3
Poli (polished)	0,1-0,2	0,02-0,1	n. d.
Plomb			
poli	0,35	0,05-0,2	n. d.
rugueux	0,65	0,6	0,4
oxydé	n. d.	0,3-0,7	0,2-0,6
Chrome	0,4	0,4	n. d.
Fer			
oxydé	0,4-0,8	0,5-0,9	0,5-0,9
non oxydé	0,35	0,1-0,3	n. d.
Rouillé (rusty)	n. d.	0,6-0,9	0,5-0,7
fondu	0,35	0,4-0,6	n. d.
Fer, versé			
oxydé	0,7-0,9	0,7-0,9	0,6-0,95
non oxydé	0,35	0,3	0,2
Fondu (melted)	0,35	0,3-0,4	0,2-0,3
Fer, forgé (forged)			
mat	0,9	0,9	0,9
Gold	0,3	0,01-0,1	n. d.
Haynes			
Alliage	0,5-0,9	0,6-0,9	0,3-0,8
Inconel			
Oxydé	0,4-0,9	0,6-0,9	0,7-,95
Abrasé (abraded)	0,3-0,4	0,3-0,6	0,3-0,6
Poli par électrolyse	0,2-0,5	0,25	0,15
Cuivre			
poli	n. d.	0,03	n. d.
rugueux	n. d.	0,05-0,2	n. d.
oxydé	0,2-0,8	0,2-0,9	0,4-0,8
Magnésium	0,3-0,8	0,05-0,3	n. d.
Laiton			
poli	0,8-0,95	0,01-0,05	n. d.
Très brillant	n. d.	n. d.	0,3
oxydé	0,6	0,6	0,5

Molybden			
oxydé	0,5-0,9	0,4-0,9	0,2-0,6
non oxydé	0,25-0,35	0,1-0,35	
Nickel			
oxydé	0,8-0,9	0,4-0,7	0,2-0,5
électrolytiquement	0,2-0,04	0,1-0,3	n. d.
Platine			
noir	n. d.	0,95	0,9
Mercure	n. d.	0,05-0,15	n. d.
Argent	n. d.	0,02	n. d.
Acier (Steel)			
Laminé à froid	0,8-0,9	0,8-0,9	0,7-0,9
Tôle brut (brut sheet metal)	n. d.	n. d.	0,4-0,6
tôle polie	0,35	0,25	0,1
Acier fusion (fusion steel)	0,35	0,25-0,4	n. d.
oxydé	0,8-0,9	0,8-0,9	0,7-0,9
inoxydable	0,35	0,2-0,9	0,1-0,8
Titane			
poli	0,5-0,75	0,3-0,5	n. d.
oxydé	n. d.	0,6-0,8	0,5-0,6
Tungstène	n. d.	0,1-0,6	n. d.
poli	0,35-0,4	0,1-0,3	n. d.
Zinc			
oxydé	0,6	0,15	0,1
poli	0,5	0,05	n. d.
Étain (non oxydé)	0,25	0,1-0,3	n. d.

n.d. : non available

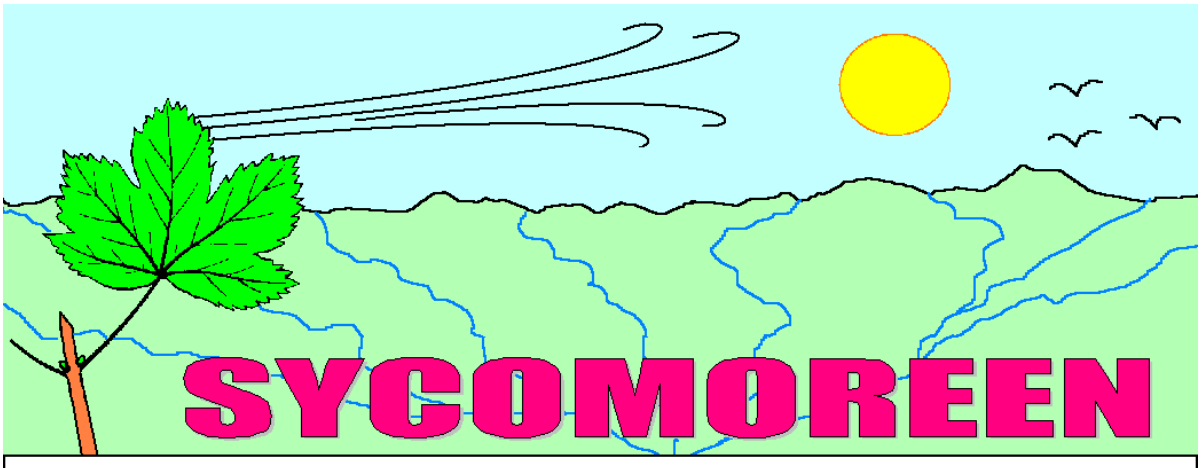

SYstems for COnversion of MOtions and REnewable ENergies
systèmes pour la conversion de mouvements et d'énergies renouvelables

El Movimiente Naturalmente Enérgico !

http://sycomoreen.free.fr